Paper:

Genetic-Algorithm-Based Fixed-Structure Robust H_∞ Loop-Shaping Control of a Pneumatic Servosystem

Somyot Kaitwanidvilai, and Manukid Parnichkun

Asian Institute of Technology
P.O.Box 4, Klong Luang, Pathumthanee, 12120, Thailand
E-mail: manukid@ait.ac.th

[Received November 20, 2003; accepted July 13, 2004]

The robust controller designed by conventional H_∞ optimal control is complicated, high-order, and difficult to implement practically. In industrial applications, structures such as lead-lag compensators and PID are widely used because their structure is simple, tuning parameters are fewer, and they are lower-order. Their disadvantages are that control parameters are difficult to tune for good performance and they lack robustness. To solve these problems, we propose an algorithm *a genetic-algorithm-based fixed-structure robust H_∞ loop-shaping control* for designing the robust controller. Conventional H_∞ loop shaping is a sensible procedure for designing the robust controller. To obtain parameters in the proposed controller, we proposed a genetic algorithm to optimize specified-structure H_∞ loop shaping problem. The infinity norm of transfer function from disturbances to states is minimized via searching and evolutionary computation. The resulting optimal parameters stabilize the system and guarantee robust performance. We applied the evolutionary robust controller to a pneumatic servosystem. To compare performance, we studied three types of controller PID with a derivative first-order filter controller, a PI controller, and an H_∞ loop-shaping controller. Results of experiments demonstrate the advantages of a simple structure and robustness against parameters changing. Simulations verify the effectiveness of the proposed technique.

Keywords: fixed-structure robust H_∞ control, H_∞ loop-shaping, genetic algorithm, pneumatic servosystem

1. Introduction

H_∞ control is a powerful technique to design robust controllers for system under conditions of uncertainty, parameter change, and disturbance. However, only robust stability alone is not enough, other performances of the controlled system such as rise time, overshoot, steady state error, etc. are also important considerations. To incorporate performance specifications into robust control, techniques such as H_2/H_∞ optimal control, the mixed sensitivity function, H_∞ loop shaping, μ-synthesis, etc., have been proposed. Most of these techniques design optimal robust controllers by solving two Riccati equations [1]. Successful practical results of H_∞ control have been shown [2–5], but controllers thus designed become have complicated structures and are high-order. Controller order depends on the order of both the nominal plant and weighting function. High order and complicated structure are not desirable in controllers to be put into practical application, however, since simpler controller often provide satisfied performance and robustness. Most of industrial applications, in fact, use simple controllers such as PI and PID, but rarely H_∞ or other complicated controllers. We present controller design of a simple structure and lower order that retains robustness. We propose fixed-structure H_∞ loop-shaping control that evolves via genetic algorithms based on the concept of H_∞ loop-shaping control proposed by Glover and McFarlane [6]. This incorporates well-known classical loop-shaping into H_∞ control problem. Controller performance is indicated by a single index, i.e., stability margin (ε) [6]. We define a controller's structure, then evaluate control parameters by genetic algorithms. We shape the nominal plant by weighting functions as is done conventionally, then define objective or fitness functions to be maximized as stability margin (ε) of the shaped plant. A high stability margin means high compatibility and robustness of the specified loop shape. Sets of controller parameters (p) in pre-specified controller ($K(p)$) are selected as individuals in the population of genetic algorithms. Based on search algorithms, natural selection, and evolution genetic algorithms are used to nonlinearly optimize specified-structure H_∞ loop-shaping optimization problem. We implement our evolutionary robust controller in a pneumatic servosystem.

The pneumatic actuator is an attractive choice in industrial and non-industrial applications over conventional electrical and hydraulic actuators due to its reliability, low cost, light weight, self-cooling, high power-to-weight ratio, etc. However, because of its inherent highly nonlinear dynamic, development of a good performance control technique for this system is difficult. Much research on the position tracking of pneumatic servosystems has used the linear or nonlinear control approach. In nonlinear control, most techniques are based on feedback lin-

earization, which transforms an algebraic nonlinear system into a linear one, so linear control is applicable. It is used to simplify models in developing robust nonlinear control such as sliding mode control [7,8]. Because it is based on a nonlinear mathematic model, it requires good knowledge in plant physics. Several experiments are required to identify nonlinear parameters such as nonlinear effective opening valve area and nonlinear friction [9]. State feedbacks such as velocity and pressure measurement are required to cancel nonlinear terms [9]. Because of time-consuming process identification and the many feedback states in the controller, this technique is implemented in applications with very precise requirements but not in general industrial applications.

In linear control, the linear model is derived from linear mathematic equations, mostly by applying linearization around a specified operation point, usually at the middle of a pneumatic cylinder. The resulting linear dynamic between position output and control valve voltage input is expressed as a third-order dynamic system, which contains a pole at the origin. Some authors [10,15] directly evaluate model parameters by measuring physical parameters. Others evaluate optimal model parameters to minimize the least square of prediction error to identify the general linear model. By assuming that a pneumatic model structure is linear and known, unknown parameters can thus be evaluated [11]. However, because of the inherent pole at the origin of the pneumatic model, it remains difficult to apply standard techniques such as the auto regressive moving average (ARMAX), auto regressive (ARX) to identify parameters. Richardson et al. [12] determined the dynamic model of a pneumatic system by applying closed-loop proportional control. They proposed a new self-tuning control for pneumatic systems. Shih et al. [13] applied a simple system identification algorithm to a pneumatic servo and reported that the accuracy of the model depended on sampling time in identification. It is difficult to specify an effective input signal for this process. Hamiti et al. [14] proposed an analog inner loop proportional controller to stabilize a pneumatic system and used a new closed-loop plant as a modified pneumatic plant model, eliminating the pole at the origin. The modified plant reduces non-linearity in pneumatic systems due to air compressibility, etc. An outer loop controller was designed to meet the performance specifications of the whole system. The modified plant model was approximated as a first-order model with time delay [14], but such a time delay is generally large, limiting the bandwidth in controller design [16]. The outer loop controller in [14] is simple and does not take robust criteria into account. In this paper, we apply an evolutionary controller at the outer loop of the pneumatic plant and an analog controller at the inner loop. In identification, we propose the approximated model as a second-order time delay model. Second-order approximation obtains more correctness than first-order approximation. Standard system identification, i.e., prediction error method [17], is used to evaluate the approximated model's parameters. The modified plant reduces some nonlinearity effects from pneumatic, so applying linear control to the modified plant is reasonable. Robust control is required to design a controller with good performance that is stable in changing plant parameters or disturbance. The proposed controller is implemented in simulation and experiments varying load mass and supplied pressure to examine the robustness of the controller's performance. This paper is organized as follows: Section 2 describes the pneumatic dynamic model, modified plant model, and identification. Section 3 presents robust control and H∞ loop shaping, detailing the proposed algorithm and fixed-structure controller that evolves by genetic algorithms. Section 4 details design, simulation, and experimental results. Section 5 summarizes and concludes the paper.

2. Pneumatic Dynamic Model and System Identification

2.1. Pneumatic Dynamic Model and Modified Plant Model

The dynamic model of a pneumatic system is difficult to determine due to its nonlinearity and large variation in plant parameters. The pole at the origin in the system also makes identification difficult. General linearization is applied at an operating point to obtain the linear dynamic model. The following mathematic model represents a pneumatic plant [14]:

$$\frac{y(s)}{u(s)} = \frac{k_1}{s(s^2 + \frac{C}{M}s + k_2)} \quad \cdots\cdots\cdots\cdots (1)$$

where

$$k_1 = \frac{\gamma R T_s G_i}{M}\left(\frac{S_p}{V_{po}} + \frac{S_n}{V_{no}}\right)$$
$$k_2 = \frac{\gamma}{M}\left(\frac{S_p^2 P_{po}}{V_{po}} + \frac{S_n^2 P_{no}}{V_{no}}\right) \quad \cdots\cdots\cdots (2)$$

where $y(s)$ is position output, $u(s)$ is the input valve voltage, γ is the ratio of specific heat $= 1.4$, S_p and S_n are areas of piston of chamber p and n, C is the viscous friction coefficient, M is piston mass, T_s is temperature, R is ideal gas constant, and V_p and V_n are the volume of chambers p and n. P_p and P_n are pressure in chambers 1 and 2. o is a subscript denoting the operation point and G_i is the coefficient of the linearized air mass flow rate. **Fig.1** shows the experimental setup of the pneumatic system.

Equation (1) shows that this model contains a pole at the origin, which complicates identification. For simplicity, a modified plant model introducing an analog proportional controller was first proposed [14]. The modified plant model is approximated as a stable plant with time delay (**Fig.2(a)**). **Fig.2(b)** shows the inner loop, outer loop, and controller. $G(s)$ is the pneumatic plant.

In the experiment, we tune proportional gain K_2 in the inner loop until a critical damp response is achieved. The following equations are derived to obtain the model of the

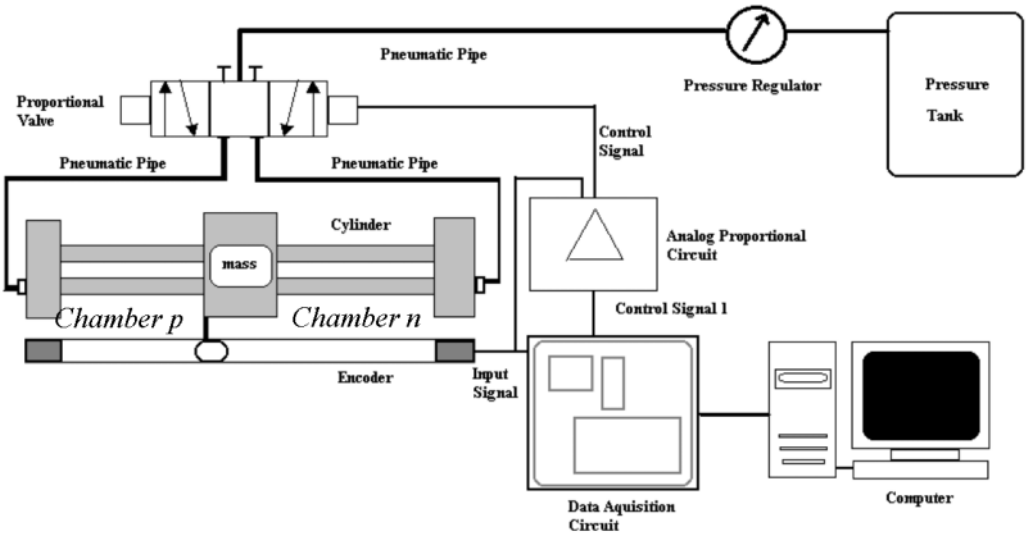

Fig. 1. Experimental setup of a pneumatic servosystem.

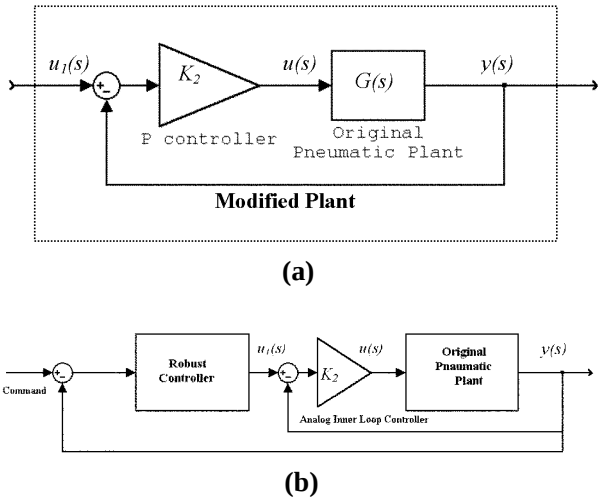

Fig. 2. (a) Modified plant model, (b) Controllers.

modified plant, whose dynamic model is, from **Fig.2(a)**:

$$y(s) = \frac{GK_2}{1+GK_2}u_1(s) = \frac{\frac{k_1K_2}{s(s^2+(C/M)s+k_2)}}{1+\frac{k_1K_2}{s(s^2+(C/M)s+k_2)}}u_1(s) \qquad (3)$$

$$\frac{y(s)}{u_1(s)} = \frac{k_1K_2}{(s^3+(C/M)s^2+k_2s+k_1K_2)} = \frac{k_1K_2}{(s+T_1)(s+T_2)(s+T_3)} \quad . \quad . \quad . \quad . \quad . \quad (4)$$

where $u_1(s)$ is a new defined input. The dynamic model in eq.(4) is approximated as a lower order model with time delay [14]. Here, we approximate the modified plant model as a second order with time delay, which is more correct than the first-order model. The following equation shows approximation of the modified plant model:

$$\frac{y(s)}{u_1(s)} \approx \frac{Ae^{-\theta_2 s}}{(s^2+b_1s+c_1)} \quad . \quad . \quad . \quad . \quad . \quad . \quad . \quad . \quad . \quad (5)$$

where θ_2 is delay time. A, b_1 and c_1 are unknown parameters that must be identified.

2.2. System Identification

System identification using experimental data is applied to determine model parameters. The model structure is known, but parameters are unknown and must be identified. The estimated model is obtained when the difference between model output, prediction, and measured output data is minimized [11]. We express the plant structure for identification in eq.(5). To identify plant parameters, we apply *the output error model (OE)*. The plant dynamic is written in the OE model as

$$y(t) = \frac{q^{-n_k}\bar{B}(q)}{F(q)}u_1(t) + e(t) \quad . \quad . \quad . \quad . \quad . \quad . \quad . \quad (6)$$

where

$$B(q) = b_{n_k}q^{-n_k} + b_{n_k+1}q^{-n_k-1} + \ldots + b_{n_k+n_b-1}q^{-n_k-n_b+1} = q^{-n_k}\bar{B}(q),$$
$$F(q) = 1 + f_1q^{-1} + f_2q^{-2} + \ldots + f_{n_f}q^{-n_f},$$

y is output, u_1 is input, e is error, n_b and n_a are the order of input and output, and n_k is time delay. The parameter vector is denoted as θ, when

$$\theta = [b_{n_k}\ b_{n_k+1}\ b_{n_k+2}\ \cdots\ b_{n_k+n_b-1}\ \ f_1\ \ f_2\ \cdots\ f_{n_f}]^T. \quad (7)$$

By applying the least square method, we identify the plant with batch data $[u_1(t), y(t)]$. Prediction error is defined as

$$\varepsilon(t,\theta) = y(t) - \hat{y}(t|\theta) \quad . \quad . \quad . \quad . \quad . \quad . \quad . \quad . \quad . \quad (8)$$

where $\hat{y}(t|\theta)$ is estimated output when parameter θ is given. The objective of identification is to find optimal

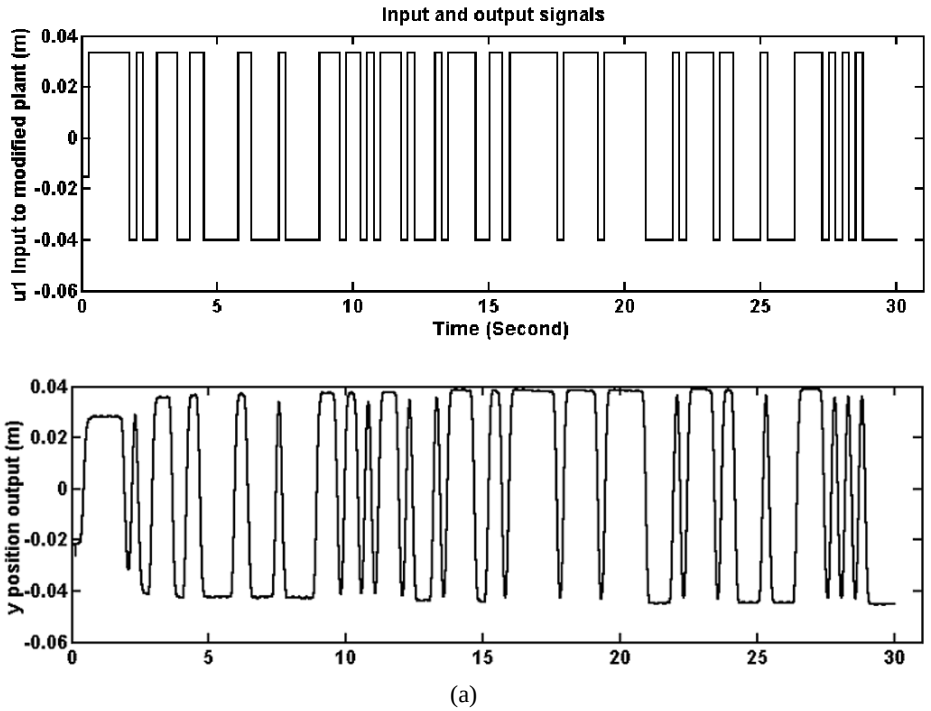

(a)

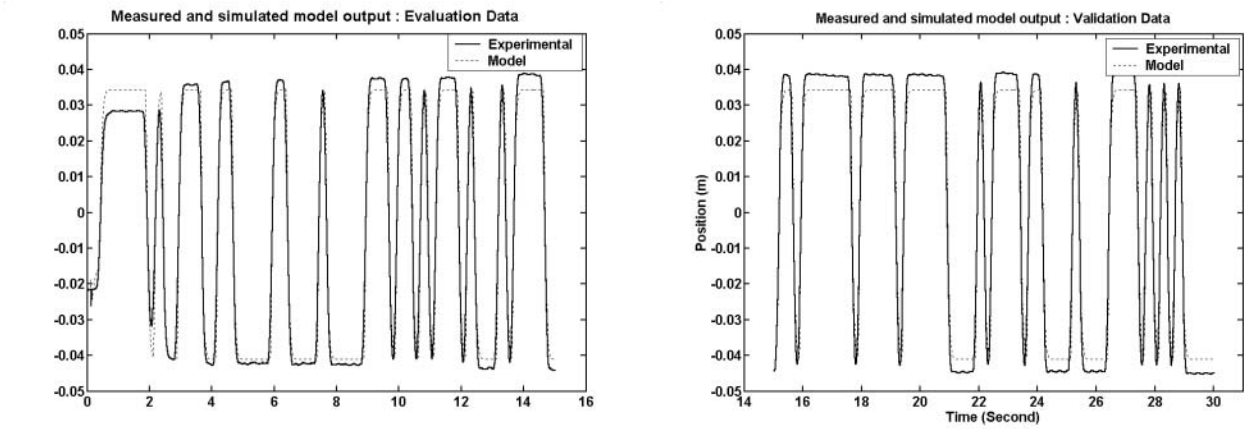

(b) Model evaluation (c) Model validation

Fig. 3. System identification. (a) Input signal $u_1(t)$ and output response $y(t)$, (b) Comparison of model and experiment, (c) Validation of model.

parameters θ that minimize the following function:

$$V = \sum_{i}^{n} \varepsilon_i(t)^2 \quad \ldots\ldots\ldots\ldots\ldots\ldots \quad (9)$$

where n is number of data set.

A continuous model of the system is obtained by transforming the discrete model into a continuous model. In our experiment, a pseudo binary random signal (PBRS) is applied as input $u_1(t)$. The time delay, 0.12 seconds, is evaluated by impulse response [17]. Sampling time in this identification is 0.01s. **Fig.3(a)** shows input signal $u_1(t)$ and output response $y(t)$. Pairs of input-output data are collected by a data acquisition circuit connected to a computer. Experimental data is divided into evaluation and validation data. Evaluation data is used to identify unknown parameters. In the experiment, we use data during 0 to 15 seconds as evaluation data. Next, we evaluate model parameters using MATLAB identification toolbox software. Validation data is used to validate the correctness of the identified model. We use data during 15 to 30 seconds as validation data. **Fig.3(b)** compares the experimental output response and its prediction model using evaluation data. **Fig.3(c)** compares validation data. Results show that the modified plant model is accurately approximated by the identified model. Through the above procedure, the identified plant model is found as

$$G_P(s) \approx \frac{551.3e^{-0.12s}}{(s^2 + 43.26s + 536.9)}. \quad \ldots\ldots\ldots \quad (10)$$

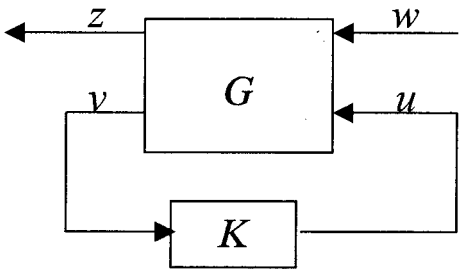

Fig. 4. General block diagram in robust control problem.

3. Genetic Algorithms Based Fixed-Structure H_∞ Loop-Shaping Control

This section details the concept of robust control synthesis by genetic-algorithm-based fixed-structure H_∞ loop shaping. Consider the system described by the block diagram (**Fig.4**), where the plant G and the controller K are real rational and proper [1]. y is output, u is control input, w is the vector signal including noises, disturbances, and reference signals, and z is the vector signal including all controlled signals and tracking errors. The H_∞ optimal control problem is *to find admission controller* $K(s)$ *such that* $\|T_{zw}\|_\infty$ *is minimized*, where $\|T_{zw}\|_\infty$ is the maximum norm of the transfer function from w to z, and the admission controller is the controller that internally stabilizes the system [1].

3.1. Conventional H_∞ Loop-Shaping Control

H_∞ loop-shaping control, proposed by McFarlane and Glover [6], is an efficient way to design a robust controller and has been applied to a variety of control problems [19–21]. Uncertainties in this approach are modeled as coprime factor uncertainty. This uncertainty model does not represent actual physical uncertainty, which, in fact, is unknown. This approach requires only a desired open loop shape in the frequency domain. Two weighting functions, W_1 (pre-compensator) and W_2 (post-compensator), are specified to shape original plant G so that the desired open loop shape is achieved. In this approach, the shaped plant is formulated as a normalized coprime factor that separates plant G_s into normalized nominator N_s and denominator M_s factors. In any plant model G, the shaped plant G_s is formulated as [6]

$$G_s = W_2 G W_1 \Rightarrow \left[\begin{array}{cc} A & B \\ C & D \end{array}\right] \quad \ldots\ldots\ldots \quad (11)$$

$$G_s = (N_s + \Delta_{N_s})(M_s + \Delta_{M_s})^{-1} \quad \ldots\ldots\ldots \quad (12)$$

where A, B, C, D represent plant G_s in the state-space form, $\left\|\Delta_{N_s}, \Delta_{M_s}\right\|_\infty \leq \varepsilon$, N_s and M_s are nominator and denominator normalized coprime factors. Δ_{N_s} and Δ_{M_s} are uncertainty transfer functions in nominator and denominator factors. ε is an uncertainty boundary, called a stability margin. To obtain these normalized coprime factors,

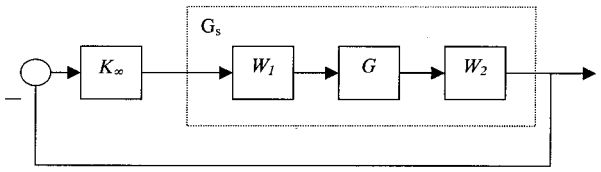

Fig. 5. Block diagram of H_∞ loop shaping.

the following equation is applied [16]:

$$[N_s \quad M_s] = \left[\begin{array}{c|ccc} A+HC & B+HD & H \\ \hline R^{-1/2}C & R^{-1/2}D & R^{-1/2} \end{array}\right] \quad . \quad (13)$$

where $H = -(BD^T + ZC^T)R^{-1}$, $R = I + DD^T$ and matrix $Z \geq 0$ is the unique positive definite solution to the algebraic Riccati equation

$$(A - BS^{-1}D^T C)Z + Z(A - BS^{-1}D^T C)^T - ZC^T R^{-1} CZ + BS^{-1}B^T = 0 \quad . \quad . \quad (14)$$

where $S = I + D^T D$.

Once the desired loop shape is achieved, the ∞-norm of the transfer function from disturbances w to states z is subjected to be minimized over all stabilizing controllers K. **Fig.5** shows the block diagram of H_∞ loop-shaping control.

3.1.1. Weighting Function Selection

Selection of the weighting function is very important in design. Fortunately, the relation between the open loop frequency domain and time domain performance is well understood [22]. This section summarizes weighting selection, detailed in [16]. Typically, we select weights W_1 and W_2 such that the open loop shaped plant has the following conflict properties:

1. Achieving good performance tracking and good disturbance rejection require large open loop gain normally at a low frequency range.
2. Achieve good robust stability and sensor noise rejection requires a small open loop gain normally at a high frequency range.

The selection of crossover frequency, i.e., the frequency at which the open loop of the shaped plant intersects with the 0dB line, is important. Practically, we select crossover frequency to achieve the desired bandwidth of our controller. The following guide explains selection:

1. For a plant with time delay θ, expected upper bound crossover frequency (w_c) must be less than $1/\theta$.
2. For a plant with a right half plan zeros (RHP), z, the expected upper bound crossover frequency (w_c) must be less than $2/z$.

3.1.2. H_∞ Loop-Shaping Design

Based on standard H_∞ loop-shaping, the following steps are proposed for an SISO plant [6]:

1. Shape singular values of nominal plant G by using pre-compensator W_1 and/or post-compensator W_2 to get the desired loop shape. W_1 and W_2 should be chosen so that G_s contains no hidden modes. W_1 is used to meet tracking performance and disturbance attenuation and W_2 to attenuate sensor noise. Practically, we select W_1 as an integral action weighting function, which make a zero steady state error. Eq.(15) shows typical weighting function W_1. W_2 can be chosen as an identity matrix because we can neglect sensor noise effect when a good sensor is used.

$$W_1 = K_w \frac{s+\alpha}{s+\delta}, \qquad W_2 = I \quad \ldots\ldots (15)$$

where K_w, α and δ are positive numbers. δ is selected as a small number $(\ll 1)$ for integral action.

2. Minimize the ∞-norm of transfer matrix T_{zw} over all stabilizing controllers K to obtain optimal cost γ_{opt}, as [1]

$$\gamma_{opt} = \varepsilon_{opt}^{-1} = \inf_{stabK} \left\| \begin{bmatrix} I \\ K \end{bmatrix} (I + G_s K)^{-1} M_s^{-1} \right\|_\infty . \quad \ldots\ldots (16)$$

The resulting ε_{opt} is a measure of robustness of the desired loop shape. It also indicates compatibility of weighting functions with robust control of the plant. $\varepsilon_{opt} < 0.25$ (or $\gamma_{opt} > 4$) indicates that W_1 or W_2 designed in step 1 is incompatible with robust stability. We must return to step (1) and readjust W_1 or W_2. ε_{opt} is determined using the unique method explained in [16]:

$$\gamma_{opt} = \varepsilon_{opt}^{-1} = (1 + \lambda_{\max}(XZ))^{1/2} \quad \ldots\ldots (17)$$

where X and Z are the solutions of Riccati equations (18) and (14), and $\lambda_{\max}$ is the maximum eigenvalue.

$$(A - BS^{-1}D^T C)^T X + X(A - BS^{-1}D^T C) - XBS^{-1}B^T X + C^T R^{-1} C = 0. \quad \ldots (18)$$

3. Select $\varepsilon < \varepsilon_{opt}$, then synthesize controller K_∞ that satisfies (negative feedback) [1,6]

$$\|T_{zw}\|_\infty = \left\| \begin{bmatrix} I \\ K_\infty \end{bmatrix} (I + G_s K_\infty)^{-1} M_s^{-1} \right\|_\infty = \left\| \begin{bmatrix} I \\ K_\infty \end{bmatrix} (I + G_s K_\infty)^{-1} [I \quad G_s] \right\|_\infty \le \varepsilon^{-1}. \quad (19)$$

Controller K_∞ is obtained by solving the optimal control problem in eq.(19).

4. Final controller (K) follows

$$K = W_1 K_\infty W_2. \quad \ldots\ldots (20)$$

3.2. Genetic-Algorithm-Based Fixed-Structure H∞ Loop-Shaping Optimization

We apply a fixed-structure robust controller. Our scope of design is an SISO plant, but it can be extended to an MIMO plant. The controller derived from direct H∞ synthesis is high-order, complicated, and not practical in actual application [23]. Fixed-structure robust controllers have becomes an interesting area of research because of their simple structure and acceptable controller order, although solving two Riccati equations as required conventionally to synthesize a fixed-structure controller remains unfeasible. We propose genetic-algorithm-based fixed-structure H∞ loop shaping to solve this problem. Although the proposed controller is structured, it retains the robustness and performance as long as satisfactory uncertainty boundary ε is achieved [24]. The proposed algorithm is as follows:

Assume predefined structure controller $K(p)$ has satisfied parameters p. The goal of optimization is to find parameters p in controller $K(p)$ that minimize infinity norm $\|T_{zw}\|_\infty$. From eq.(20), controller $K(p)$ is written as

$$K(p) = W_1 K_\infty W_2 \quad \ldots\ldots (21)$$

or

$$K_\infty W_2 = W_1^{-1} K(p). \quad \ldots\ldots (22)$$

We select weight $W_2 = I$, which implies that sensor noise is negligible and not considered. Thus,

$$K_\infty = W_1^{-1} K(p). \quad \ldots\ldots (23)$$

By substituting eq.(23) into eq.(19), the ∞-norm of the transfer function matrix from disturbance to state, $\|T_{zw}\|_\infty$, which is minimized, is written as shown in eq.(24). $\|T_{zw}\|_\infty$ is used as cost function J_{cost} of the genetic algorithm.

$$J_{cost} = \gamma = \|T_{zw}\|_\infty = \left\| \begin{bmatrix} I \\ W_1^{-1} K(p) \end{bmatrix} (I + G_s W_1^{-1} K(p))^{-1} [I \quad G_s] \right\|_\infty . \quad \ldots\ldots (24)$$

Although the infinity norm is difficult to calculate, powerful mathematic software such as MATLAB provides functions to evaluate this norm.

Genetic algorithms are well known as a biologically inspired class of algorithms applicable to any nonlinear optimization problem. This algorithm applies the concept of chromosomes and the operations of crossover, mutation, and reproduction. A chromosome is an individual sample in a population. Each individual is assigned a fitness based on evaluation and objective functions. At each step, called generation, fitness values of all individuals in a population are calculated. Individual with maximum fitness value is retained as a solution in the current generation and passed to the next generation. To form a new population of the next generation, crossover, mutation, and reproduction are used. Crossover randomly selects a site along the length of two chromosomes, then splits the two chromosomes at the crossover site. New chro-

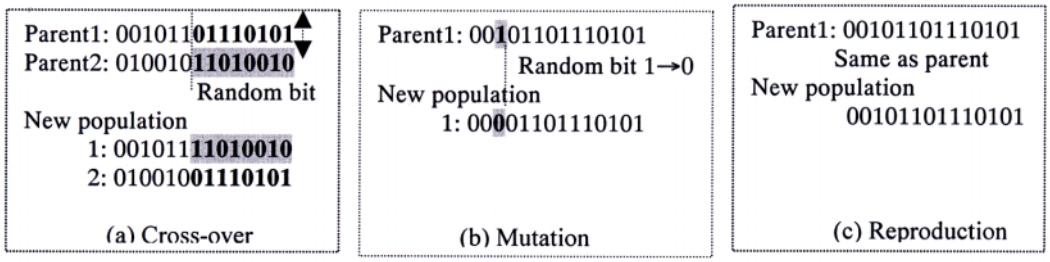

Fig. 6. Genetic operations. (a) Crossover, (b) Mutation, and (c) Reproduction.

mosomes are then formed by matching the head of one chromosome with the tail of the other. Mutation forms a new chromosome by randomly changing a single bit in the chromosome. Reproduction forms a new chromosome by copying the old chromosome. Chromosome selection in genetic algorithms depends on the fitness value. High fitness means a high chance of being selected. Mutation, reproduction, or crossover depends on the pre-specified operation's probability. Individual samples in the genetic population are coded in binary. For real numbers, decoding binary to floating-point numbers is used [25]. The following example illustrates the coding procedure. Assume that $p = [K_p, K_i]$ as the parameters of PI controller. The range of parameters are assume as $0.0 \leq K_p \leq 5.0$, $0.0 \leq K_i \leq 10.0$. The number of bits in a parameter is assumed as 10, therefore, K_p and K_i can be coded as the following.

K_p	**code**		K_i	**code**
0.00000	0000000000		0.00000	0000000000
0.00488	0000000001		0.00977	0000000001
0.00977	0000000010		0.01955	0000000010
	⋮		⋮	⋮
5.00000	1111111111		10.0000	1111111111

For example, p = [0.00977, 10.0000] is code as [0000000101111111111]. Crossover, mutation, and reproduction are shown in **Fig.6**. The algorithm is summarized as follows:

Steps 1 and 2 Apply the McFarlane and Glover procedure [16]. $\varepsilon_{opt} < 0.25$ (or $\gamma_{opt} > 4$) indicates that W_1 and W_2 are incompatible with robust stability. W_1 or W_2 is adjusted.

Step 3 Select controller structure $K(p)$ and initialize several sets of parameters p as the population in the first generation. Define genetic parameters such as initial population size, crossover and mutation probability, and maximum generation.

Step 4 Evaluate cost function, J_{cost}, of each individual using eq.(24). Assign $J_{cost} = 100$, or a large number if $K(p)$ does not stabilize plant G. Select the individual with minimum cost as a solution in the current generation. For the first generation, Gen = 1.

Step 5 Increment the generation by 1 step.

Step 6 While the current generation is less than the maximum generation, create new population using genetic operators and go to step 4. If the current generation is the maximum generation, stop.

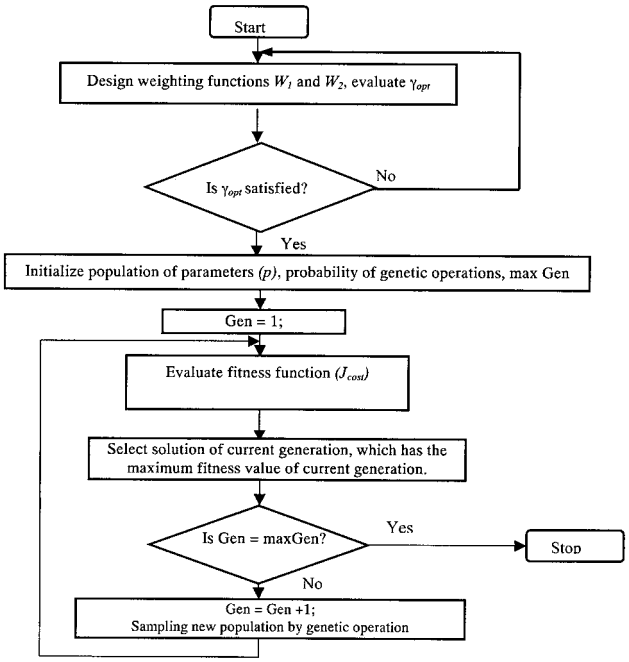

Fig. 7. Flow chart of design.

Step 7 Check performances in frequency and time domains. If performance is unsatisfactory, such as too low ε, go to step 1 to change weighting functions or control structure. Low ε indicates that weighting functions and/or selected control structure is not suitable to the problem. Other properties in the time domain such as overshoot and rise time are also important. **Fig.7** shows the flow of the proposed algorithm.

4. Simulation, Experiments, and Results for Pneumatic System

From identification in Section 2.2, the modified nominal plant is modeled as a second-order model with time delay. We approximate the delay term in the model by a first-order Pade's approximation. The identified plant

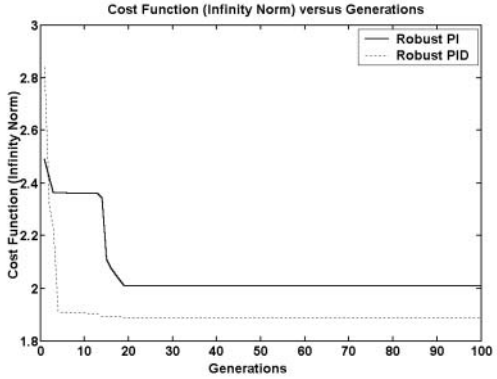

Fig. 8. Cost functions J_{cost} versus iteration in genetic algorithm.

model is thus

$$G_P(s) \approx \frac{551.3e^{-0.12s}}{(s^2+43.26s+536.9)} = \frac{551.3(-0.06s+1)}{(s^2+43.26s+536.9)(0.06s+1)} \quad \ldots (25)$$

where the first-order Pade's approximation is

$$e^{-\theta s} \approx \left(\frac{-\frac{\theta}{2}s+1}{\frac{\theta}{2}s+1}\right). \quad \ldots (26)$$

In the model, crossover frequency must not exceed $1/\theta$, 8.33rad/s. Weighting functions are selected using the guideline in [16]. W_1 is an integral action weighting function, small positive pole, to conduct a zero steady state error. Identity W_2 is selected because sensor noise is assumed to be negligible. According to eq.(15), we select weighting functions as

$$W_1 = \frac{0.75s+4.0}{s+0.001}, \quad W_2 = 1. \quad \ldots (27)$$

With these weighting functions, the bandwidth of the desired control system is about 4.0rad/s. These weighting functions significantly improve performance and robustness.

For comparison, we evaluated different controllers. We first design a controller by conventional H∞ loop-shaping, then transform the transfer function of the shaped plant to a state-space form as follows:

$$G_s = W_1 G W_2 = \frac{0.75s+4.0}{s+0.001}\frac{551.3(-0.06s+1)}{(s^2+43.26s+536.9)(0.06s+1)}$$

$$\Rightarrow \left[\begin{array}{cc} A & B \\ C & D \end{array}\right]$$

$$\Rightarrow \left[\begin{array}{cccc|c} -59.9 & -19.7 & -4.36 & -0.00 & 4.0 \\ 64.00 & 0.000 & 0.000 & 0.000 & 0.0 \\ 0.000 & 32.00 & 0.000 & 0.000 & 0.0 \\ 0.000 & 0.000 & 8.000 & 0.000 & 0.0 \\ \hline 0.000 & -1.62 & 0.572 & 0.561 & 0.0 \end{array}\right]. \quad \ldots (28)$$

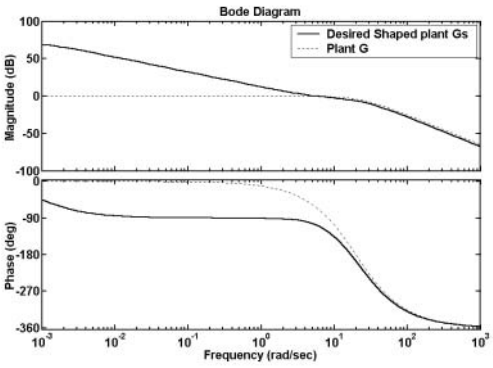

(a) Loop shape of plant and desired shape plant

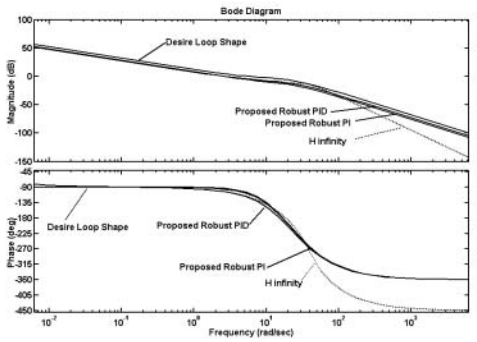

(b) Desired loop shape and loop shape by conventional H infinity loop shaping, proposed PI, and proposed PID controllers

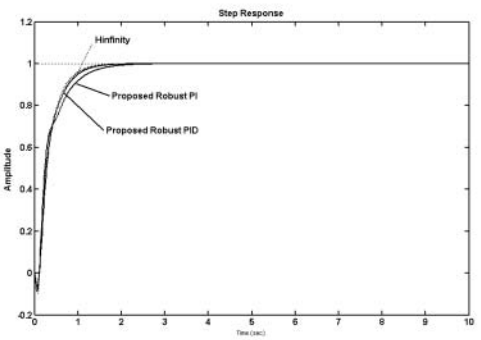

(c) Step responses of proposed PI, PID and H infinity controllers

Fig. 9. Bode diagram of (a) plant and shaped plant, (b) desired loop shape and loop shape by proposed controllers, and (c) step responses of controllers.

By solving eqs.(14), (17), and (18), optimal stability margin ε_{opt} is found to be 0.5793. In conventional H∞ loop-shaping, we select $\varepsilon = 0.5475$, less than the optimum value. Solving eq.(19), controller K_∞ is obtained as follows:

$$K_\infty(s) = \frac{44.9329(s+16.67)(s^2+41.8s+470.2)}{(s+61.04)(s+5.64)(s^2+36.13s+1561)}. \quad \ldots (29)$$

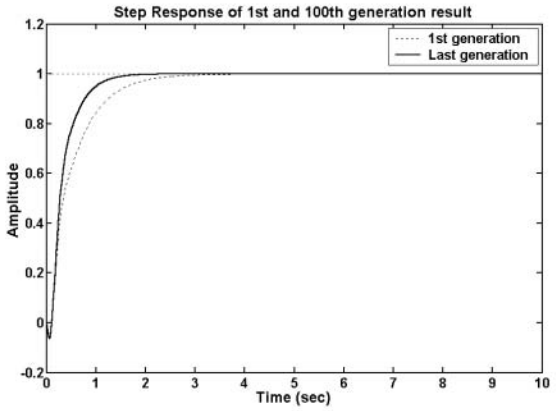

Fig. 10. Comparison of step responses of controller after first and 100th generations of proposed PID controller.

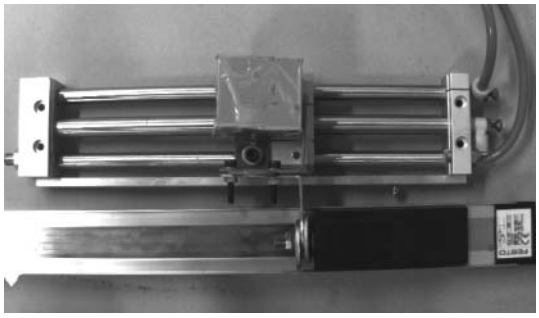

Fig. 11. Pneumatic actuator system and encoder.

With eq.(20), we obtain the conventional H_∞ loop-shaping controller as follows:

$$K(s) = W_1 K_\infty W_2 = \frac{(0.75s+4.0)}{s+0.001} \times \frac{44.9329(s+16.67)(s^2+41.8s+470.2)}{(s+61.04)(s+5.64)(s^2+36.13s+1561)} = \frac{33.6996(s+16.67)(s+5.333)(s^2+41.8s+470.2)}{(s+61.04)(s+5.64)(s+0.001)(s^2+36.13s+1561)}. \quad (30)$$

The controller in eq.(30) is fifth-order and complicated, making it difficult to implement practically.

We try PID with a derivative first-order filter controller as the fixed-structure controller. The controller structure is expressed in eq.(31). K_p, K_i, K_d, and τ_d are parameters to be evaluated.

$$K(p) = K_p + \frac{K_i}{s} + \frac{K_d s}{\tau_d s+1}. \quad (31)$$

We select controller parameters, their ranges, and genetic algorithms parameters as follows: $K_p \in [0.0, 10.0]$, $K_i \in [0.0, 10.0]$, $K_d \in [0.0, 1.0]$, $\tau_d \in [0.0, 20.0]$, population size $= 500$, crossover probability $= 0.9$, mutation probability $= 0.1$, maximum generation $= 100$, and number of bits that represent one parameter $= 24$. 100 generations are run by genetic algorithm. The obtained optimal solution is shown in eq.(32), which has a stability margin of 0.5298 (or $\gamma = 1.8875$).

$$K(p) = 0.2356 + \frac{2.5017}{s} + \frac{0.7298s}{12.6007s+1}. \quad (32)$$

We try a fixed-structure PI controller. The optimal solution is shown in eq.(33), which has a stability margin of 0.4975 (or $\gamma = 2.0101$).

$$K(p) = 0.4083 + \frac{2.369}{s}. \quad (33)$$

Figure 8 shows plots of convergence of cost function J_{cost}, the inverse of the stability margin, versus generations by genetic algorithm. Both optimal fixed-structure controllers provide a satisfied stability margin at 0.5298 and 0.4975 for PID with a derivative first-order filter and PI, respectively.

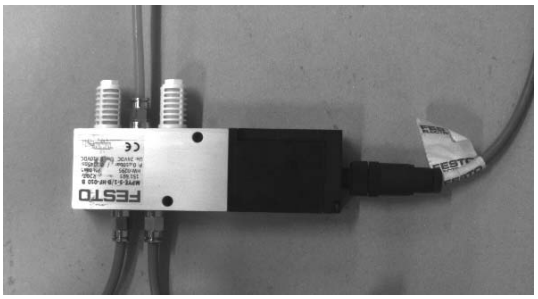

Fig. 12. Proportional valve.

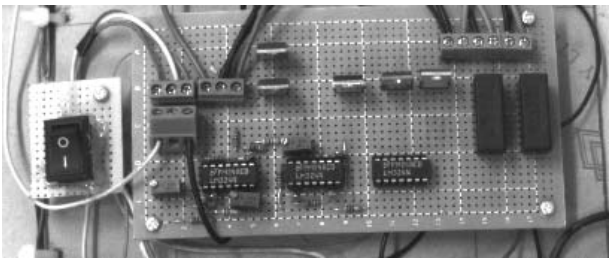

Analog proportional circuit

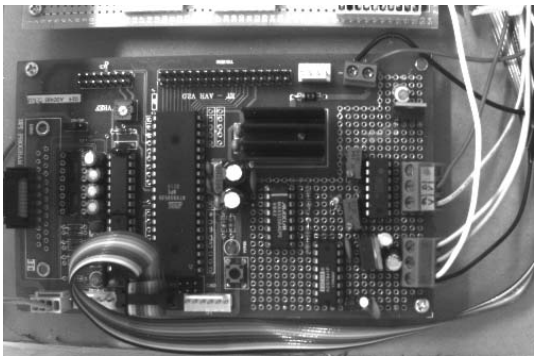

Data acquisition circuit

Fig. 13. Analog proportional controller and data acquisition circuit.

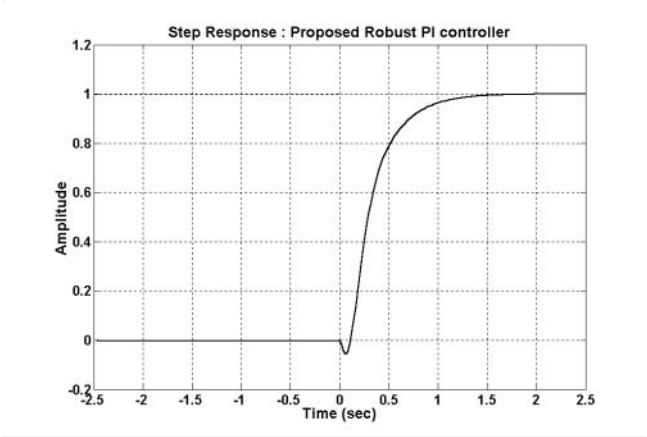

(a) Simulation result

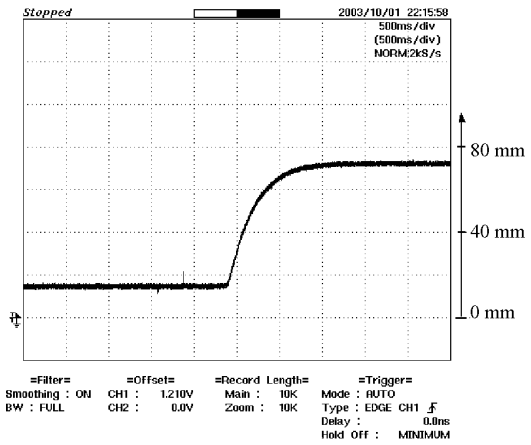

(b) Experimental result

Fig. 14. (a) Simulation result, and (b) Experimental result of proposed optimal robust PI controller (Scale: Y-axis: 20mm/division, X-axis: 0.5s/division).

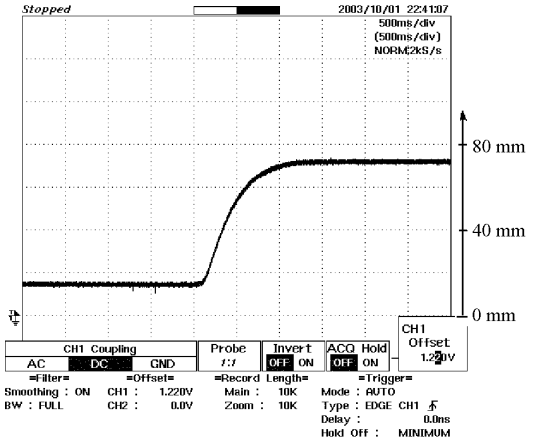

Fig. 15. Step response at 400kPa supply pressure (nominal supply pressure = 550kPa) (Scale: Y axis: 20mm/division, X axis: 0.5s/division).

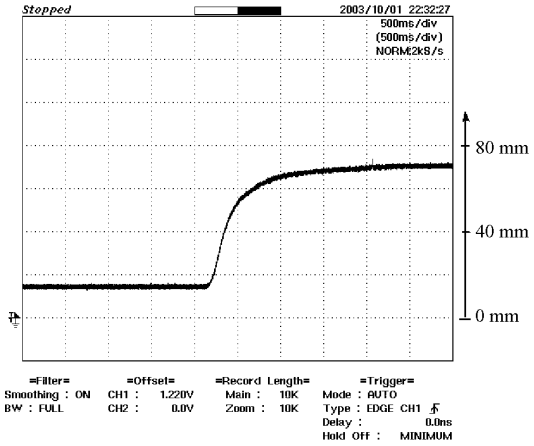

Fig. 16. Step response at 3kg load mass (nominal load = 1kg) (Scale: Y axis: 20mm/division, X axis: 0.5s/division).

Open loop bode diagrams are plotted to verify proposed algorithms. **Fig.9(a)** compares plant G and specified shaped plant G_s. The desired loop shape and the loop shape by the proposed controller are plotted in **Fig.9(b)**. It is clearly shown that the proposed technique performs as robust controller, which corresponds to the desired loop shape. Both loop shapes of PI and PID with a derivative first-order filter are close to the desired loop shape. **Fig.9(c)** shows step responses of the optimal solution from the proposed robust PI, PID with a derivative first-order filter, and the conventional H_∞ controller.

Figure 10 compares step responses in the controller after the first and 100^{th} generations, showing that the genetic algorithm improves performance in the time domain and in robustness.

The experiment is done on a 200mm, low friction pneumatic cylinder, SMC CDY1S10H, which has 700kPa rated pressure. The 5-port proportional valve used in the experiment is Festo MPYE-5-1/8-HF-010B, which has -700 to 700ℓ/min flow. A linear potentiometer, Festo-POT-500L, is used as a position sensor. Nominal supply pressure is maintained at a constant 550kPa by a pressure regulator. **Figs.11-13** show equipment used in the experiment. **Fig.14** shows simulation and experimental results of the step response of the proposed robust PI controller in eq.(33). Results are similar, showing overly damp responses and about the same rise time. The simulation result has no steady state error. In the experimental result, the steady state error is about ± 0.3mm due to a non-model friction dynamic, dead-zone of valve, and limitation of sensor resolution.

We conducted other experiments to verify the robustness of the proposed controller. First, we changed the supply pressure of the pneumatic system, equivalent to parameter variation in the nominal plant. We also changed load mass. Both experimental results show that the proposed controller has good robust performance from supply pressure uncertainty and load mass. Responses are overly damp with small different in rise-time. **Figs.15** and **16** show the results of step response in changing supply pressure and load mass.

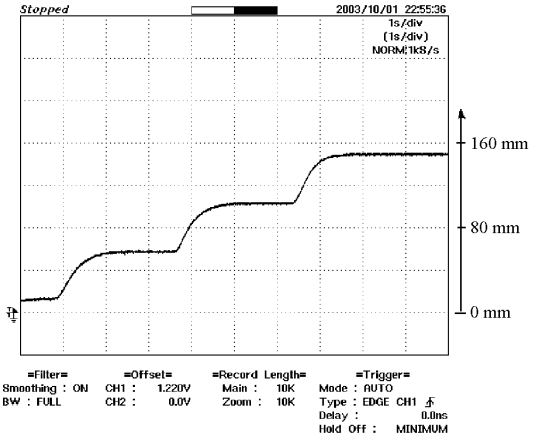

Fig. 17. Response at different location on pneumatic cylinder (Scale: Y axis: 40mm/division, X axis: 1.0s/division).

Figure 17 shows experimental results of the proposed controller at different locations on the cylinder, indicating that the proposed controller is applicable to a wide range of operations.

5. Conclusion

The proposed controller achieves good robust performance by applying two specified weighting functions. Although design of a fixed-structure controller is difficult because of its inherently non-convex nonlinear problem, the genetic algorithm simplifies this by searching for optimal solutions. Based on the concept of convention H_∞ loop shaping, only a single index, stability margin, ε, is applied to indicate performance of the designed controller. Optimal stability margin ε_{opt} is found to be 0.5793 for conventional H_∞ loop shaping. We then choose $\varepsilon = 0.5475$ to design the robust controller. The controller obtained from conventional H_∞ loop shaping is high-order and complicated. For proposed PI and PID control with a derivative first-order filter, optimal solutions of ε after running genetic algorithms for 100 generations are 0.4975 and 0.5298, respectively, indicating that designed controllers are compatible with the specified open loop shape and also guarantee robustness. In the frequency response, the conventional H_∞ loop-shaping controller performs closer to the desired loop shape than the proposed technique. However, because of the complicated controller in the conventional design, the proposed approach significantly improves practical control by simplifying the controller structure and reducing the controller order while retaining robust performance. This makes the proposed controller more practical and attractive. Experimental results show the robust performances of the proposed controller. Changing load mass and supply pressure has little effect on the controlled output response.

In conclusion, by combining the two approaches of genetic algorithms and H_∞ loop shaping; we designed a fixed-structure controller. Although this approach cannot guarantee an invariably satisfactory solution, in most cases, the solution exists. Implementation in a pneumatic system confirmed that the proposed technique is valid and flexible. Other control performances will be considered in further research with multiple objective functions.

References:

[1] K. Zhou, and J. C. Doyle, "Essential of Robust Control," Prentice-Hall, 1998.

[2] Y.-C. Chu, K. Gloverb, and A. P. Dowlingb, "Control of combustion oscillations via H_∞ loop-shaping," μ-analysis and Integral Quadratic Constraints, Automatic, Vol.39, pp. 219-231, 2003.

[3] T. Kimura, S. Hara, and T. Takamori, "H_∞ control with Mirror Feedback for a Pneumatic Actuator System," Proceeding of 35th Conference on Decision and Control, Kobe, Japan, December 1996.

[4] T. Kimura, H. Fujioka, K. Tokai, and T. Takamori, "Sampled-data H_∞ control for a pneumatic cylinder system," Proceeding of 35th Conference on Decision and Control, Kobe, Japan, December 1996.

[5] J. H. Park, "H-Infinity Direct Yaw Moment Control with Brakes for Robust Performance and Stability of Vehicles," JSME International Journal, Series C, Vol.44, No.2, pp. 403-413, 2001.

[6] D. C. McFarlane, and K. Glover, "A loop shaping design procedure using H_∞ synthesis," IEEE Trans. On Automatic Control AC-37 (6), pp. 759-769, 1992.

[7] A. K. Paul, J. K. Mishra, and M. G. Radke, "Reduced Order Sliding Mode Control for Pneumatic Actuator," IEEE Transection On Control Systems Technology, Vol.2, No.3, September 1994.

[8] J. Song, and Y. Isnida, "A Robust control for pneumatic servo system," Int. Journal of Engineering Science, Vol.35, No.8, pp. 711-723, 1997.

[9] F. Xiang, and J. Wikander, "Block-oriented approximate feedback linearization for control of pneumatic actuator system," Control Engineering Practice, In Press, Corrected Proof, Available online 31 May 2003.

[10] W. Backe, and O. Ohligschlaeger, "Model of heat transfer in pneumatic chambers," Journal of Fluid Control, Vol.20, No.1, pp. 61-78, 1989.

[11] L. Ljung, "System Identification: Theory for the User," Prentice-Hall 2nd edition, 1999.

[12] R. Richardson, A. R. Plummer, and M. D. Brown, "Self-Tuning Control of a Low-Friction Pneumatic Actuator Under the Influence of Gravity," IEEE Transactions on Control Systems, Vol.9, No.2, March 2001.

[13] M.-C. Shih, and S.-I. Tseng, "Identification and Position Control of a Servo Pneumatic Cylinder," Control Engineering Practice, Elsevier Science, Vol.3, No.9, pp. 1285-1290, 1995.

[14] K. Hamiti et al., "Positin Control of A Pneumatic Actuator Under the Influence of Stiction," Control Engineering Practice, Elsevier Science, Vol.4, No.8, pp. 1079-1088, 1996.

[15] M. Uebing, and N. D. Maughan, "On linear modeling of a pneumatic servo system," Proceeding of the Fifth Scandinavian International Conference on Fluid Power, Vol.2, pp. 363-378, Linkoping, Sweden, 1997.

[16] S. Skogestad, and I. Postlethwaite, "Multivariable Feedback Control Analysis and Design," John Wiley & Son, 1996.

[17] MATLAB System Identification Toolbox, Mathworks co., Ltd., http://www.mathworks.com.

[18] T. Virvalo, "Designing a Pneumatic Positionc Servo System," Power International, 1989.

[19] S. Ibaraki, and M. Tomizuka, "Tuning of a Hard Disk Drive Servo Controller Using H_∞ Fixed-Structure Controller Optimization," Journal of Dynamic Systems, Measurement, and Control, Vol.123, September 2001.

[20] Y.-C. Chu, K. Gloverb, and A. P. Dowlingb, "Control of combustion oscillations via H_∞ loop-shaping," μ-analysis and Integral Quadratic Constraints, Automatica 39, pp. 219-231, 2003.

[21] X.-D. Sun, P. G. Scotson, and G. Balfour, "A Further Application of Loop Shaping H-infinity Control to Diesel Engine Control – Driven-Idle Speed Control," SAE Technique paper series, SAE 2002 World Congress, Detroit, Michiganm, March 4-7, 2002.

[22] B. J. Lurie, and P. J. Enright, "Classical Feedback Control with MATLAB," Marcel Dekker, Inc., pp. 94-129, 2000.

[23] B.-S. Chen, and Y.-M. Cheng, "A Structure-Specified optimal Control Design for Practical Applications: A Genetic Approach," IEEE Trans. on Control System Technology, Vol.6, No.6, November 1998.

[24] B.-S. Chen, Y.-M. Cheng, and C.-H. Lee, "A Genetic Approach to Mixed H_2/H_∞ Optimal PID Control," IEEE Trans. on Control Systems, pp. 51-60, 1995.

[25] C. Houck, J. Joines, and M. Kay, "A Genetic Algorithm for Function Optimization: A MATLAB Implementation," by NCSU-IE TR 95-09, 1995.

Name:
Somyot Kaitwanidvilai

Affiliation:
Asian Institute of Technology, School of Advanced Technologies, Mechatronics

Address:
P.O.Box 4, Klongluang, Pathumthani 12120 Thailand

Brief Biographical History:
1997- Assistant Researcher, NECTEC, Thailand
2000- Lecturer, Naresuan University, Thailand

Main Works:
- S. Kaitwanidvilai, and M. Parnichkun, "Active Baysian Feature Weighting in Reinforcement Learning Robot," IEEE International Conference on Industrial Technology, 2002.
- S. Kaitwanidvilai, and W. Khan-ngern, "The Analysis of Deadtime Effect on Unbalanced Load for Three Phase PWM Inverters," International Power Electronic Conference 2000, Tokyo, Japan, April 3-7, 2000.

Name:
Manukid Parnichkun

Affiliation:
Asian Institute of Technology, School of Advanced Technologies, Mechatronics

Address:
P.O.Box 4, Klongluang, Pathumthani 12120 Thailand

Brief Biographical History:
1996- Assistant Professor, Asian Institute of Technology
2001- Associate Professor, Asian Institute of Technology

Main Works:
- "Geometric and Force Errors Compensation in a 3-axis CNC Milling Machine," International Journal of Machine Tools & Manufacture, Elsevier Science Ltd., Vol.44/12-13, pp. 1283-1291, 2004.
- "Kinematics Control of a Pneumatic System by Hybrid Fuzzy PID," International Journal of Mechatronics, Elsevier Science Ltd., Pergamon, Vol.11, No.8, pp. 1001-1023, 2001.

Membership in Learned Societies:
- Thai Robotics Society